

Microwave Network Study by Bond Graph Approach. Application to Tow-Port Network Filter

Sabri Jmal^{1†} and Hichem Taghouti^{2††} and Abdelkader Mami^{3†},

[†]University of Tunis El Manar, Faculty Of Sciences Of Tunis, Tunis, Tunisia. ^{††}Carthage University, Higher institute of environment sciences and technologies Borj Cedria, Tunisia.

Summary

There are much processing techniques of microwave circuits, whose dimensions are small compared to the wavelength, but the disadvantage is that they cannot be directly applied to circuits working at high and/or low frequencies. In this article, we will consider the bond graph approach as a tool for analyzing and understanding the behavior of microwave circuits, and to show how basic circuit and network concepts can be extended to handle many microwaves analysis and design problems of practical interest. This behavior revealed in the scattering matrix filter, and which will be operated from its reduced bond graph model. So, we propose in this paper, a new application of bond graph approach jointly with the scattering bond graph for a high frequency study.

Key words:

Bond Graph Approach; Scattering Formalisme; Microwave Filter; Scattering Parameter, Network.

1. Introduction

Bond graph approach [1] is a graphic language unified for all the fields of the engineering. It confirmed like a structured approach with the modeling and the simulation of the multi-field systems. It gives a structural analysis [2] and a concise description of the simple or complex linear or not linear systems in the shape of half arrows carrying the power variables couple of effort (e : often noted \mathcal{E} in its reduced form) and flow (f : often noted φ in its reduced form), of elements with simple junctions characterizing the nodes with effort or common flow, of elements with balanced junctions consisted by transformers and gyrators and allowing the coupling between the various under-parts of a physical system with a power transfer without losses, of the passive elements transforming the power which is provided to them in dissipated or stored energy.

Moreover, the development of bond graph technique was articulated around two basic concepts with knowing the reticulation assumption and the principle of power continuity [3].

Whereas the scattering formalism [4], which results in a matrix noted ‘‘S’’, is the basic tool for the

circuits and components study in microwave and in lines theory [5] in a biggest domain going from a very low frequencies to highest. It includes explicitly the conservation laws and respects, in an intrinsic way, the causal relations through its various properties [6].

We propose in this paper to apply this graphic approach jointly with the scattering formalism and we will consider it like a new tool and solution for the comprehensive and analysis of the HF circuits and network antennas. To understand the behavior of microwave systems [7] (network antennas and/or HF circuits) we will exploit its scattering parameters (S_{ij}), for that, we will present an analytical operating procedure of these scattering parameters (Scattering Matrix ‘‘S’’) [8]. This procedure will be applicate to the reduced and causal bond graph model of HF network filter.

2. Generalities on the Scattering Formalism

Since the definition of the boundaries of a physical system is needed during its modeling, the crosslinking hypothesis introduced by PAYNTER [17], allows us to suppose that it is possible to separate and locate the properties of the physical object that is the given system and thus to define the object as a set of basic properties connected.

2.1 Waves Variables in 2-Port Network

We consider two 2-Port Network ‘‘SYS1 and SYS2’’ interacting and communicating with each other as shown in Figure 1. The SYS1 and SYS2 represent two elements each of which has two ports through which it communicates. The connection between these two elements is done through a simple link represents interconnection that interaction.

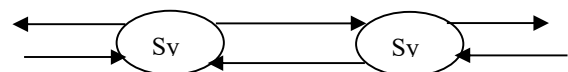


Fig. 1. A cascade connection of tow 2-port Networks

Based on the assumption of the power continuity [18 ;19] and the concept of energy conservation which is provided by a flow of energy between elements, we can say that the

relationship linking **SYS1** and **SYS2** shows the same energy flow and can associate a common size noted **P** (instantaneous power) which is the product of two conjugate variables: **e** noted the effort and the flow **f** noted that are used in all energy fields.

$$P(t) = e(t) * f(t) \tag{1}$$

The **P** power can be expressed in the following form:

$$P = P_{12} - P_{21} \tag{2}$$

Where:

P_{12} : Power circulates from **SYS1** to **SYS2**.

P_{21} : Power circulates from **SYS2** to **SYS1**.

Based on the assumption made by **PAYNTER** and **BUSCH-Vishniac** [17] can be associated to each of the two powers **P₁** and **P₂**, a positive scalar which can be defined by the following expressions:

$$P_{12} = \frac{w_{i2}^2}{2} \tag{3}$$

$$P_{21} = \frac{w_{21}^2}{2} \tag{4}$$

With: W_{12} : The wave circulates from **SYS1** to **SYS2**

W_{21} : The wave circulates from **SYS2** to **SYS1**

The link connecting the **SYS1** and **SYS2** in Figure 1 can be broken down for each system into two branches. Each branch represents either the incident W_i or the reflected W_r wave shown in Figure 2.

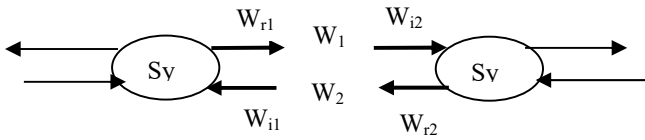


Fig. 2. Scattering representation of 2-Port Network

W_{11} and W_{12} incident waves associated with input signals.

W_{r1} and W_{r2} reflected waves associated with output signals.

The W_{12} and W_{21} waves are the vibration amplitudes of the corresponding waves. This concept is introduced into the scattering formalism [20; 21; 17].

If now both **SYS1** and **SYS2** systems are coupled, the assumption of the power of continuity [17;19] can give us:

$$w_{i1} = w_{21} = w_{r2} \tag{5}$$

$$w_{r1} = w_{12} = w_{i2} \tag{6}$$

The universality of application of scattering formalism allows linking W_r and W_i waves to the usual variable's effort and flow. That's why we can report that the power **P** flowing in the link connecting the two systems **SYS1** and **SYS2** is written as a product of two intrinsic variables noted: \mathcal{E} (intrinsic variable: effort) and φ

(intrinsic variable: flow) from the linear transformation developed by **Breedveld** [18].

$$P = \frac{w_{i2}^2}{2} - \frac{w_{r2}^2}{2} = \mathcal{E} \cdot \varphi \tag{7}$$

$$\begin{pmatrix} w_{i2} + w_{r2} \\ \sqrt{2} \end{pmatrix} \begin{pmatrix} w_{i2} - w_{r2} \\ \sqrt{2} \end{pmatrix} = \mathcal{E} \cdot \varphi \tag{8}$$

From equation 8, we can write the following linear transformation:

$$\begin{bmatrix} \mathcal{E} \\ \varphi \end{bmatrix} = \frac{1}{\sqrt{2}} \begin{bmatrix} 1 & 1 \\ 1 & -1 \end{bmatrix} \begin{bmatrix} w_{i2} \\ w_{r2} \end{bmatrix} = H \begin{bmatrix} w_{i2} \\ w_{r2} \end{bmatrix} \tag{9}$$

The matrix equation indicated by the equation below represents the passage variable effort and intrinsic flow (\mathcal{E}, φ) to variable wave (W_i, W_r) through an inverse linear transformation of the transformation ‘**H**’.

$$\begin{bmatrix} w_i \\ w_r \end{bmatrix} = \frac{1}{\sqrt{2}} \begin{bmatrix} 1 & 1 \\ 1 & -1 \end{bmatrix} \begin{bmatrix} \mathcal{E} \\ \varphi \end{bmatrix} = H^{-1} \begin{bmatrix} \mathcal{E} \\ \varphi \end{bmatrix} \tag{10}$$

The matrix ‘**H**’ is orthogonal view that there is equality between this matrix and its inverse.

2.2 Scattering Representation

Generally, characterization of any linear network can be achieved by linear-algebraic differential equations that interconnect the variable force and flow of the various pairs of ports in the network. Depending on the nature of the problem, these equations can be used in various forms since they result from the use of Ohm's law and Kirchhoff-constitutive relationships of the elements. We can define the **Z** impedance matrices and **Y** admittance, which according **BELEVITCH** [22 ; 23] may not exist unlike representation scattering, arranging the complex coefficients network features in a table or matrix, this is done by the use of transformational computing and grouping of similar variables in a vector.

Considering now any linear system with n-ports characterized by \mathcal{E} and φ variables as shown in the figure below:

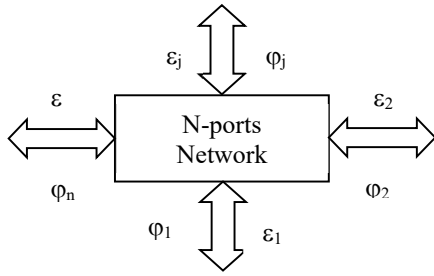


Fig. 3. Linear System with N-Ports

In the context of the scattering representation, the n-ports linear system represented by Figure 3 will be characterized by the wave variables as shown in the following figure:

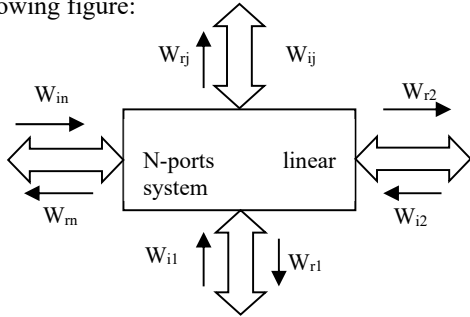


Fig. 4. Characterization of an N-ports Network with wave variables

The variables of incident waves and reflected waves shown in the above figure are written in the general form:

$$\begin{bmatrix} w_{r1} \\ w_{r2} \\ \vdots \\ w_{rn} \end{bmatrix} = \begin{bmatrix} S_{11} & S_{12} & \cdots & S_{1n} \\ \vdots & S_{22} & & \vdots \\ \vdots & & \ddots & \vdots \\ S_{n1} & \cdots & S_{nj} & \cdots & S_{nn} \end{bmatrix} \begin{bmatrix} w_{i1} \\ w_{i2} \\ \vdots \\ w_{in} \end{bmatrix} \quad (11)$$

Or :

$$[w_r] = [S][w_i] \quad (12)$$

The diagonal elements of the ‘‘S’’ matrix denote the reflection coefficients while the non-diagonal elements designate the transmission coefficients. All these factors are called scattering parameters and are constituted by a linear combination of algebraic or differential operators [12;13;14].

3. Analytical Procedure Exploitation

Either the linear system with 2N-port indicated by the following figure, it comprises n-ports to the input and n-ports to the output.

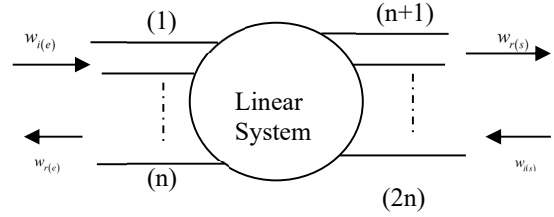


Fig. 5. Linear System with 2N-Ports

As shown in the above figure, the incident and reflected waves at 2n-ports will be broken down into two groups: those entries ($w_{i(e)}, w_{r(e)}$) and other ($w_{i(s)}, w_{r(s)}$) for outputs.

These 2n waves are bound by 2n relationships matrix expressing the relationship between the inputs waves and outputs waves through the system.

$$\begin{bmatrix} w_{i(e)} \\ w_{r(e)} \end{bmatrix} = W \begin{bmatrix} w_{i(s)} \\ w_{r(s)} \end{bmatrix} \quad (13)$$

The W matrix may take another form as before by breaking down into four square matrices of order n as shown in the following expression:

$$\begin{bmatrix} w_{i(e)} \\ w_{r(e)} \end{bmatrix} = \begin{bmatrix} W_{11} & \vdots & W_{12} \\ \cdots & \cdots & \cdots \\ W_{21} & \vdots & W_{22} \end{bmatrix} \begin{bmatrix} w_{i(s)} \\ w_{r(s)} \end{bmatrix} \quad (14)$$

Whereas a succession of two simple physical systems rated respectively (p) and (p+1). The incident and reflected waves to inputs of the system ports (p) are respectively $w_{i(e)}^p$ and $w_{r(e)}^p$, while $w_{i(s)}^p$ and $w_{r(s)}^p$ are the incident and reflected waves to the output ports of the same system.

$W^{(p)}$, the wave matrix can, then, be written according to the following relationship:

$$\begin{bmatrix} w_{i(e)}^{(p)} \\ w_{r(e)}^{(p)} \end{bmatrix} = W^{(p)} \begin{bmatrix} w_{i(s)}^{(p)} \\ w_{r(s)}^{(p)} \end{bmatrix} \quad (15)$$

In the same manner and for the system (p+1) we see that $w_{i(e)}^{(p+1)}$ and $w_{r(e)}^{(p+1)}$ are respectively the incident and reflected waves at the ports of entries of this system while its incident and reflected waves at the ports outputs are respectively $w_{i(s)}^{(p+1)}$ and $w_{r(s)}^{(p+1)}$, so, we can writing the wave matrix $W^{(p+1)}$.

$$\begin{bmatrix} w_{i(e)}^{(p+1)} \\ w_{r(e)}^{(p+1)} \end{bmatrix} = W^{(p+1)} \begin{bmatrix} w_{i(s)}^{(p+1)} \\ w_{r(s)}^{(p+1)} \end{bmatrix} \quad (16)$$

Generally, the chain of m systems to input and output n -ports gives us a system equivalent to n -port input and global wave array output W_T .

$$W_T = W^{(1)} \cdot W^{(2)} \dots W^{(m)} = \prod_{p=1}^m W^{(p)} \quad (17)$$

If making a partition of S scattering matrix into four square matrices with 'n' order corresponding to the two port groups (inputs and outputs) we can have:

$$\begin{bmatrix} W_{r(e)} \\ W_{r(s)} \end{bmatrix} = \begin{bmatrix} S_{11} & \vdots & S_{12} \\ \dots & \dots & \dots \\ S_{21} & \vdots & S_{22} \end{bmatrix} \begin{bmatrix} W_{i(e)} \\ W_{i(s)} \end{bmatrix} \quad (18)$$

By taking into account the equation 2, we can write all possible combinations between the components of the scattering matrix and the matrix of the wave components:

$$\begin{cases} S_{11} = -\frac{W_{12}}{W_{22}} \\ S_{12} = \frac{1}{W_{22}} \\ S_{21} = \frac{W_{22} \cdot W_{11} - W_{12} \cdot W_{21}}{W_{22}} \\ S_{22} = \frac{W_{21}}{W_{22}} \end{cases} \quad (19)$$

And

$$\begin{cases} W_{11} = \frac{S_{22}}{S_{21}} \\ W_{12} = \frac{1}{S_{21}} \\ W_{21} = \frac{S_{21} \cdot S_{12} - S_{22} \cdot S_{11}}{S_{21}} \\ W_{22} = \frac{S_{11}}{S_{21}} \end{cases} \quad (20)$$

4. Scattering Formalism Exploiting from Bond Graph Approach

4.1 Reduced bond graph transformation

Generally the reduced bond graph model is the result of a certain number of transformations which consist in normalization, compared to a chosen normalization resistance, the elements with simple junction structure (junction 0 and junction 1), the elements with balanced junction (junction TF and junction GY) and the energy storage elements (inductance L and capacity C) and the dissipation (resistance R) of such kind that the variable

effort and flows (e and f) are replaced by the noted reduced variables (\mathcal{E}, φ) [8] as the following figure indicates it.

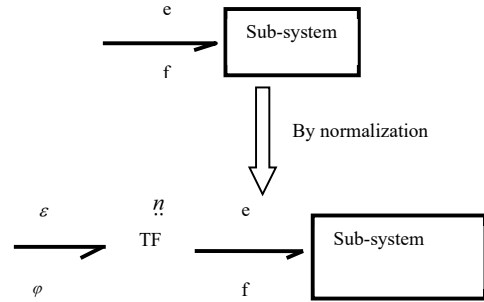


Fig. 6. Normalization of 2-Ports Network.

$$n = \frac{1}{\sqrt{R_0}} \quad (21)$$

The power variables defined above may be written in another form, considering the relationship of the transformer.

$$\mathcal{E} = \frac{e}{\sqrt{R_0}} \quad (22)$$

$$\varphi = f \cdot \sqrt{R_0} \quad (23)$$

R_0 represents the standard real and positive resistance.

4.2 Scattering parameters Exploitation

The causality assignment to the reduced bond graph model of figure 6 enables us to notice that they are four different cases of causality assignment in input-output of the process [8]. For each case, there is one equation which connects the reduced variables effort and flows (of the entry and/or exit) to the other reduced variables and to the algebraic-graph operators H_{ij} ($i, j=1 \dots 2$) associated with the causal ways and determined by using the Masson rule [7].

$$H_{ij}(s) = \frac{\sum_i L_{ij}(s) \Delta_{ij}(t)}{\Delta(s)} \quad (24)$$

Where:

Δ : is the determinant of bond graph model defined by

$$\Delta = 1 - \sum B_i + \sum B_i B_j - \sum B_i B_j B_k \quad (25)$$

$\sum B_i$: The sum of the earnings of individual loops.

$\sum_{B_i B_j}$: is the sum of the products of pairs of loops gains not touching, etc.

Δ_{ij} : is the reduced determinant extract from Δ by removing the loops touching the input-output causal path.

L_{ij} : The transmittance of the path from j to i.

The four cases of causality assignment are given by the following figures.

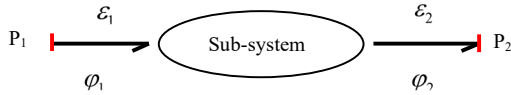


Fig. 7. The flow-flow causality assignment

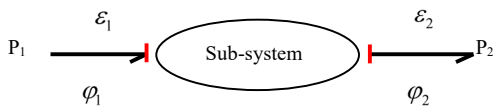


Fig. 8. The effort-effort causality assignment

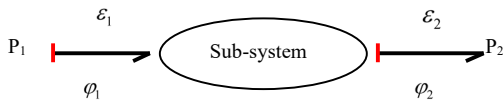


Fig. 9. The flow-effort causality assignment

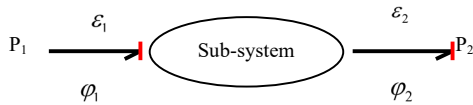


Fig. 10. The effort-flow causality assignment

From these different causality assignments, we can find these different equations.

Table 1 Scattering matrices associated with the various cases of causality assignment

Different cases of causality	S-matrix
Case 1 : Causality flow-flow	With: $\Delta H = H_{11}H_{22} - H_{12}H_{21}$ and $D = 1 + H_{11} - H_{22} - \Delta H$ $S = \frac{1}{D} \begin{bmatrix} -1 + H_{11} + H_{22} - \Delta H & -2H_{12} \\ 2H_{21} & -1 - H_{11} - H_{22} - \Delta H \end{bmatrix}$
Case 2 : Causality effort-effort	$S = \frac{1}{D} \begin{bmatrix} 1 - H_{11} - H_{22} + \Delta H & -2H_{12} \\ 2H_{21} & 1 + H_{11} + H_{22} + \Delta H \end{bmatrix}$
Case 3 : Causality flow-effort	$S = \frac{1}{D} \begin{bmatrix} -1 + H_{11} + H_{22} - \Delta H & 2H_{12} \\ 2H_{21} & 1 + H_{11} + H_{22} + \Delta H \end{bmatrix}$
Case 4 : Causality effort-flow	$S = \frac{1}{D} \begin{bmatrix} 1 - H_{11} - H_{22} + \Delta H & 2H_{12} \\ 2H_{21} & -1 - H_{11} - H_{22} - \Delta H \end{bmatrix}$

5. Application to 2-Port Network

5.1 Network with localized elements

we propose to apply the previously analytical operation method for a high frequency filter based on localized elements [9] and which has 10Ghz of cut-off frequency, this filter is interposed between endpoints [10;11] which are only P₁ and P₂ ports as shown in the following figure.

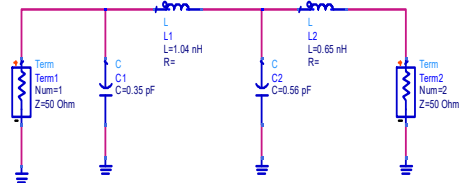


Fig. 11. 2-Port Network Filter with localized elements

The causal and conventional bond graph model of this filter interposed between the two ports P₁ and P₂ is given below.

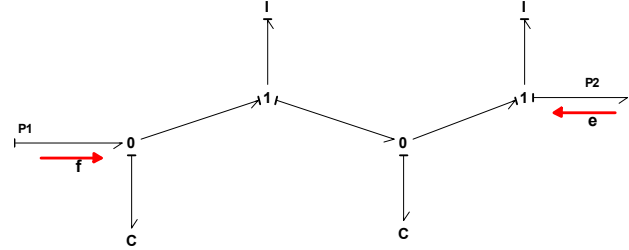


Fig. 12. Bond graph model of the filter

From this model, we can get the causal and reduced bond graph model indicated by the figure below, and after reducing its elements by performing processing by connecting an ideal transformer to each port of the constituent elements of this model [24; 25].

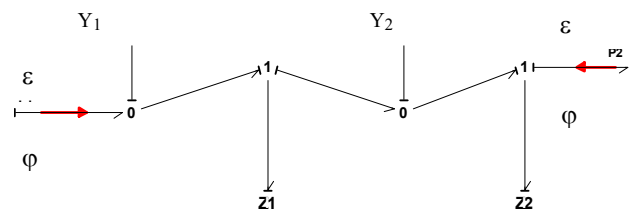


Fig. 13. Reduced bond graph model

This bond graph model has a particular structure, hence the need for an additional step before the implementation of the operating procedure of scattering parameters. This step consists of inserting junction (0 or 1) decomposition [24; 26] following the bond graph model considered to break it down into two sub-systems without change or causality of the constituent elements of the system. This step we therefore facilitate the implementation of the operating procedure for the calculating of the scattering matrix.

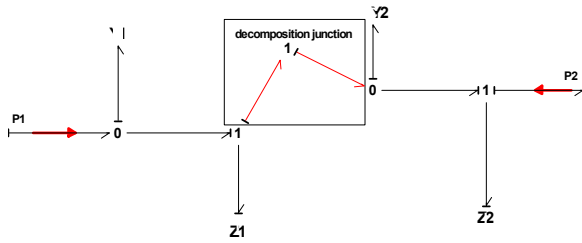


Fig. 14. Reduced bond graph model with decomposition junction

The breakdown of the bond graph model according to decomposition junction 1 give us two subsystems whose reduced and causal bond graph models are shown in the following figure:

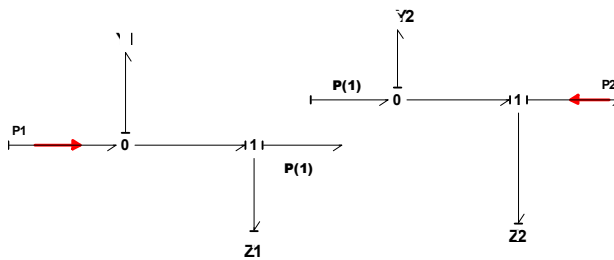


Fig. 15. The tow reduced bond graph sub-model after decomposition

$z_1 = \tau_{L1} \cdot s$: reduced impedance of L_1 element

$z_2 = \tau_{L2} \cdot s$: reduced impedance of L_2 element

$y_1 = \tau_{C1} \cdot s$: reduced admittance of C_1 element

$y_2 = \tau_{C2} \cdot s$: reduced admittance of C_2 element

$$\tau_{C1} = C_1 \cdot R_0 \text{ and } \tau_{C2} = C_2 \cdot R_0 \quad (26)$$

$$\tau_{L1} = L_1 / R_0 \text{ et } \tau_{L2} = L_2 / R_0 \quad (27)$$

Walking through the two reduced bond graph sub-models, we note the existence of a single causal loop model for every penny and whose associated integro-differential operator is:

$$B_1 = \frac{-1}{z_1 y_2} \text{ and } B_2 = \frac{-1}{z_2 y_1} \quad (28)$$

The integro differential operators are:

$$\Delta_1 = 1 + \frac{1}{z_1 y_1} \text{ and } \Delta_2 = 1 + \frac{1}{z_2 y_2} \quad (29)$$

From the first sub-model we can write:

$$\begin{cases} H_{11} = \frac{z_1}{z_1 y_1 + 1} \\ H_{12} = \frac{1}{z_1 y_1 + 1} \\ H_{21} = \frac{1}{z_1 y_1 + 1} \\ H_{22} = \frac{-y_1}{z_1 y_1 + 1} \\ \Delta H = \frac{-1}{z_1 y_1 + 1} \end{cases} \quad (30)$$

From the second sub-model:

$$\begin{cases} H_{11} = \frac{z_2}{z_2 y_2 + 1} \\ H_{12} = \frac{1}{z_2 y_2 + 1} \\ H_{21} = \frac{1}{z_2 y_2 + 1} \\ H_{22} = \frac{-y_2}{z_2 y_2 + 1} \\ \Delta H = \frac{-1}{z_2 y_2 + 1} \end{cases} \quad (31)$$

However, as the S matrix is not ‘‘cascadable’’, we can determine the wave matrix for each sub-model and then apply it the expression of equation 7 for the overall wave matrix bond graph model reduces full electrical filter.

For the first sub-model:

$$W^{(1)} = \frac{1}{2} \begin{bmatrix} z_1 y_1 - z_1 - y_1 + 2 & -z_1 y_1 + z_1 + y_1 \\ -z_1 y_1 - z_1 + y_1 & z_1 y_1 + z_1 + y_1 \end{bmatrix} \quad (32)$$

And for the second one:

$$W^{(2)} = \frac{1}{2} \begin{bmatrix} z_2 y_2 - z_2 - y_2 + 2 & -z_2 y_2 + z_2 + y_2 \\ -z_2 y_2 - z_2 + y_2 & z_2 y_2 + z_2 + y_2 \end{bmatrix} \quad (33)$$

The total wave matrix is:

$$W^{(T)} = W^{(1)} \cdot W^{(2)} = \begin{bmatrix} W_{11} & W_{12} \\ W_{21} & W_{22} \end{bmatrix} \quad (34)$$

From the overall wave and matrix found by referring to the expression of equation 18, we can determine the parameters of the scattering matrix as follows:

$$S_{11} = \frac{\tau_{C1} \tau_{C2} \tau_{L1} \tau_{L2} s^4 + \tau_{L1} \tau_{C2} (\tau_{C1} - \tau_{L2}) s^3 + [\tau_{C1} (\tau_{L2} + \tau_{L1}) + \tau_{C2} (\tau_{L2} - \tau_{L1})] s^2 + (\tau_{C1} + \tau_{C2} - \tau_{L1} - \tau_{L2}) s}{\tau_{C1} \tau_{C2} \tau_{L1} \tau_{L2} s^4 + \tau_{L1} \tau_{C2} (\tau_{C1} + \tau_{L2}) s^3 + (\tau_{C1} + \tau_{C2}) (\tau_{L1} + \tau_{L2}) s^2 + (\tau_{C1} + \tau_{C2} + \tau_{L1} + \tau_{L2}) s + 2}$$

$$S_{22} = \frac{-\tau_{C1} \tau_{C2} \tau_{L1} \tau_{L2} s^4 + \tau_{L1} \tau_{C2} (\tau_{C1} - \tau_{L2}) s^3 + [\tau_{C2} (\tau_{L1} + \tau_{L2}) - \tau_{C1} (\tau_{L1} + \tau_{L2})] s^2 + (\tau_{C1} + \tau_{C2} - \tau_{L1} - \tau_{L2}) s}{\tau_{C1} \tau_{C2} \tau_{L1} \tau_{L2} s^4 + \tau_{L1} \tau_{C2} (\tau_{C1} + \tau_{L2}) s^3 + (\tau_{C1} + \tau_{C2}) (\tau_{L1} + \tau_{L2}) s^2 + (\tau_{C1} + \tau_{C2} + \tau_{L1} + \tau_{L2}) s + 2}$$

$$S_{21} = \frac{2}{\tau_{C1} \tau_{C2} \tau_{L1} \tau_{L2} s^4 + \tau_{L1} \tau_{C2} (\tau_{C1} + \tau_{L2}) s^3 + (\tau_{C1} + \tau_{C2}) (\tau_{L1} + \tau_{L2}) s^2 + (\tau_{C1} + \tau_{C2} + \tau_{L1} + \tau_{L2}) s + 2}$$

$$S_{12} = \frac{2}{\tau_{C1} \tau_{C2} \tau_{L1} \tau_{L2} s^4 + \tau_{L1} \tau_{C2} (\tau_{C1} + \tau_{L2}) s^3 + (\tau_{C1} + \tau_{C2}) (\tau_{L1} + \tau_{L2}) s^2 + (\tau_{C1} + \tau_{C2} + \tau_{L1} + \tau_{L2}) s + 2}$$

5.2 Simulation results and comparison study

The simulation of the previous equations given bellow

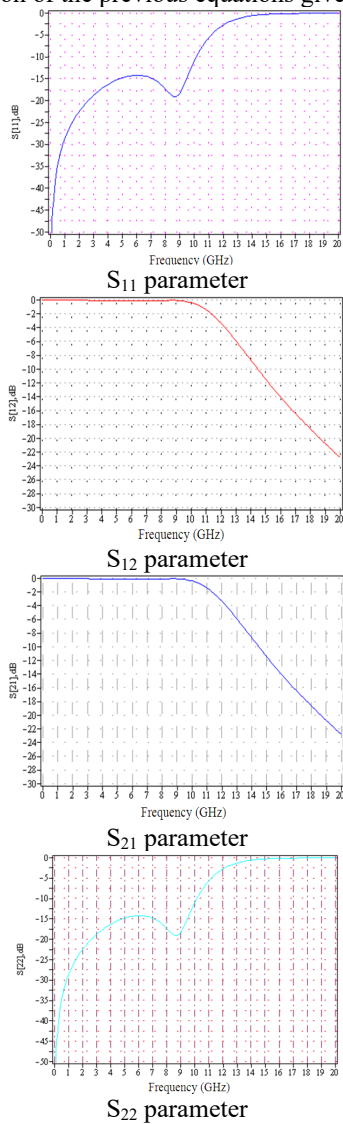


Fig. 16. Scattering parameters representation

Validation of results is performed by the simulation of the electrical circuit of the digital simulation software HP-ADS used in microwave.

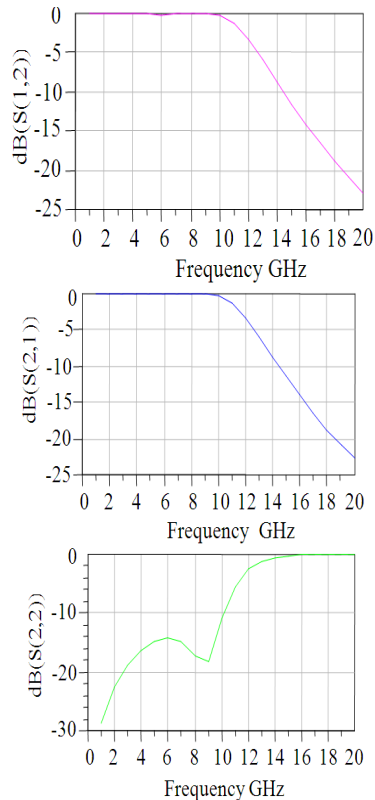
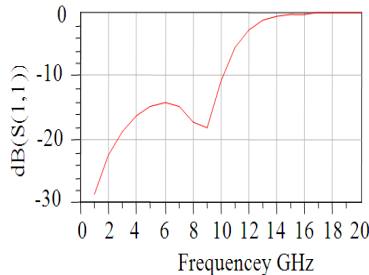


Fig. 17. Simulation of the network filter by HP-ADS

The objective of these simulations is the validation of the technique used to operate the scattering parameters from the causal bond graph model of the filter and operating in high frequency unlike the work of A. Kamel [15;16] where the concept of causality was ignored despite it represents a significant ownership in the network type of formalism and particularly the bond graph formalism.

All simulations of figure 16 were performed under the Maple software to show us the shape of the reflection coefficient (S₁₁ and S₂₂) and transmission (S₁₂ and S₂₁) which, in turn, give us information concerning the type and order of the filter and its cutoff frequency. While the simulation data in figure 17 and which were carried out directly under the HP-ADS software to validate the simulations of figure 16.

6. Conclusion

We can say that this systematic procedure has two advantages; the first is the superposition of the two formalisms and systematic transition from one to the other using the concepts of causal path and causal loop. The second interest is the fact that this method allows to simultaneously study a given system with two formalisms that are complementary which promotes a wider understanding of its behavior.

From this section, input the body of your manuscript according to the constitution that you had. For detailed information for authors, please refer to [1].

Acknowledgments

We would like to acknowledge all members of Laboratory of Analysis, Design and Control Systems without forgetting all researchers of High frequency electronic circuits and systems Laboratory (05/UR/11-10). We note that this project is supported by ENIT; LR11ES20.

References

- [1] Karnopp D.C., Margolis D. L., Rosenberg R.C. "System dynamics: Modeling and simulation of mechatronic systems", John Wiley & Sons Inc., New York, 2005.
- [2] D. Karnopp and R.C.Rosenberg, "Analysis and simulation of multiport Systems-The bond Graph Approach to physical system Dynamics" The MIT Press, 1968.
- [3] C. Sueur and G. Dauphin-Tanguy, "Bond graph approach for structural analysis of MIMO linear systems", J. Franklin Inst., Vol. 328, No. I, pp. 55-70, 1991.
- [4] Ferrero Andrea, Pirola Marco, "Generalized Mixed-Mode S-Parameters", IEEE Transactions on Microwave Theory and Techniques , Vol.54, No. I, p.p. 458-463, 2006.
- [5] Jia Sheng Hong, M J Lancaster, Waun Ed Hong, "Microstrip filters for RF/microwave applications", ISBN: 0471388777, EAN: 9780471388777, No. of Pages: 488, Jun 2001.
- [6] V. Belevich, "Classical Network Theory" Holden-Day, San Francisco, 1968.
- [7] Kubiak Philippe, "Analyse Symbolique des Systèmes physiques Modelises par bond graph et Comportant des Eléments Multiports ", These de Doctorat, N° : 96 LIL1 0218, 1996.
- [8] M. Amara and S. Scavarda, "A Procedure to Match Bond Graph And The Formalism Scattering" J. of Franklin Inst., Vol. 328, N° 516, pp. 887-889, 1991.
- [9] Cao, Y., Wang, G., & Zhang, Q. J. (2009). "A new training approach for parametric modeling of microwave passive components using combined neural networks and transfer functions". Microwave Theory and Techniques, IEEE Transactions on, 57(11), 2727-2742.
- [10] Taghouti, H., & Mami, A. (2012). "Discussion around the Scattering Matrix Realization of a Microwave Filter using the Bond Graph Approach and Scattering Formalism". American Journal of Applied Sciences, 9(4).
- [11] Hichem Taghouti and Abdelkader Mami, "New Extraction Method Of The Scattering Parameters Of A Physical System Starting From Its Causal Bond Graph Model: Application To A Microwave Filter", Int. J. Phys. Sci. Vol.6 (13), pp. 3016-3030.July2011. DOI:10.5897/IJPS10.216.
- [12] Borutzky, W. (2011). "Bond Graph Modelling of Engineering Systems" (pp. 4-10). Springer.
- [13] Taghouti, H., Mami, A., & Jmal, S. (2014). "Nouvelle Technique de Modélisation et Simulation par Bond Graph: Applications aux Circuits Hauts Fréquences et Antennes Patch". Éditions universitaires européennes.
- [14] Proakis, J. G., Salehi, M., Zhou, N., & Li, X. (1994). "Communication systems engineering", Vol. 2. Englewood Cliffs: Prentice-hall.
- [15] KAMEL, A. et DAUPHIN-TANGUY, G. "Power transfer in physical systems using the scattering bond graph and a parametric identification approach Source Systems", Analysis Modelling Simulation. Vol. 27, Issue 1, p. 1 – 13. 1996.
- [16] KAMEL, A., SUEUR C. et DAUPHIN-TANGUY, G. "How to Derive a Bond Graph Model from a Transfer Matrix", J. of the Franklin Inst., Vol. 330, N° 5, pp. 787-798, 1993.
- [17] PAYNTER, H.M., ILENE J. et BUSCH-VISHNIAC "Wave scattering approaches to conservation and causality", J. Franklin inst. 1988, Vol. 325, N° 3, pp. 295-313.
- [18] BREEDVELD, P. C. "Multi-bond graph elements", J. Franklin. Inst. Jan/Feb. 1985, Vol. 319, pp. 1-36.
- [19] BREEDVELD, P.C., ROSENBERG, R.C. et ZHOU, T. "Bond Graph Bibliography", J. of Franklin Inst., Vol. 328, N° 5/6, pp. 1067-1109, 1991.
- [20] Jmal, S., Taghouti, H., & Mami, A. 2014. "Modeling and simulation of a patch antenna from its Bond Graph model". International Conference on Control, Decision and Information Technologies (CoDIT), 2014 (pp. 609-614). IEEE.
- [21] Jmal, S., Taghouti, H., & Mami, A. 2013. "A new modeling and simulation methodology of a patch antenna by Bond Graph approach". International Conference on Electrical Engineering and Software Applications (ICEESA), 2013 (pp. 1-6). IEEE.
- [22] BELEVITCH, V. "Classical Network Theory", Holden-Day, San Francisco, 1968.
- [23] Taghouti, H. and A. Mami, 2010. "Modeling Method of a Low-Pass Filter Based on Microstrip T-Lines with Cut-Off Frequency 10 GHz by the Extraction of its Wave-Scattering Parameters from its Causal Bond Graph Model". Am. J. Eng. Applied Sci., 3: 631-642.
- [24] AMARA, M. et SCAVARDA, S. "A Procedure to Match Bond Graph and the Scattering Formalism", J. of the Franklin Inst., Vol. 328, N° 516, pp. 887-899, 1991.
- [25] Hichem Taghouti, Sabri Jmal and Abdelkader Mami, "Joint use of Bond Graph Approach and Scattering Formalism for an Electrical Modeling of Patch Antenna Array", Research Journal of Applied Sciences, Engineering and Technology, 11(2): 135-143.
- [26] Sabri Jmal, Hichem Taghouti, Abdelkader Mami, "Design of a Ka Band Antenna by a New Methodology Based on Bond Graph Approach". International Journal on Communications Antenna and Propagation (IRECAP),5(5):pp.301-306, 2015References

Sabri JMAL, received the B.E. and M.E. degrees, from Tunis Elmanar Univ. in 2010 and 2012, respectively. He received the Dr. Eng. degree from ElManar universit in 2017. His research interest includes simulation and modeling of antennas by a new methodology named scattering bond graph. He is a member of laboratory of energy in faculty of sciences of tunis.